Design of LLC Resonant Tank in a Low Power DC/DC Power Converter

Katarina Obradović, Emilija Lukić, Jovana Plavšić and Aleksandar Milić

***Abstract*— Photovoltaic power conversion prosperity has put a spotlight on the resonant DC/DC converters. Namely, improved power density and lessened power losses can be achieved due to its soft switching feature. Step by step design procedure of the LLC resonant tank is proposed in this paper. Analysis of the parameters of the tank, capacitor selection and a detailed inductor design are demonstrated thoroughly. Finally, experimental results of the developed 1000 W DC/DC converter with suggested LLC resonant configuration are presented.**

***Index Terms*— DC/DC converter, LLC resonant tank, high frequency, capacitor selection, inductor design**

I. Introduction

Increased interest in the use of renewable energy sources has inspired the development of new solutions in power electronics. Its unprecedented expansion has resulted in continued advances regarding power conversion's efficiency, safety, as well as the price.

Since photovoltaic (PV) systems represent DC power source, in order to successfully connect them to AC power grid, the use of switching power converters is inevitable. With aspirations to achieve better efficiency of power conversion, Maximum Power Point Tracking (MPPT) algorithm needs to be implemented in a DC/DC stage of the device. Possible topologies include non-isolated converters such as boost, buck, buck-boost or Ćuk topology presented in [1] - [4] and isolated configurations like flyback, push-pull, and resonant converters [5] - [8]. Furthermore, in a MPPT stage soft switching can be achieved and high frequency employed [9].

High frequency resonant converters accommodate great qualities such as improved safety with galvanic isolation, absence of high switching losses thanks to zero current (ZCS) and zero voltage switching (ZVS), along with better power density due to reduced volume of the magnetic components [10] [11].

Katarina Obradović is member of Department of Power Converters and Drives, University of Belgrade, 73 Bulevar kralja Aleksandra 73, 11020 Belgrade, Serbia (e-mail: obradovick15@gmail.com).

Emilija Lukić is member of Department of Power Converters and Drives, University of Belgrade, 73 Bulevar kralja Aleksandra 73, 11020 Belgrade, Serbia (e-mail: emilija.lukic505@gmail.com).

Jovana Plavšić is member of Department of Power Converters and Drives, University of Belgrade, 73 Bulevar kralja Aleksandra 73, 11020 Belgrade, Serbia (e-mail: plavsicjovana37@gmail.com).

Aleksandar Milić is with the School of Electrical Engineering, University of Belgrade, 73 Bulevar kralja Aleksandra, 11020 Belgrade, Serbia (e-mail: milic.aleksandar@etf.bg.ac.rs).

Numerous resonant tank configurations are possible such as parallel, series or a combination of both resonant phenomenon [12]. The voltage gain of a series resonant configuration (SRC) can take a maximum of 1, while a parallel resonant converter (PRC) can achieve up to 10. Three and four reactive energy storage elements that combine parallel and series resonant phenomenon are more stable for a wide range of loads, and additionally parasitic inductances or capacitances featured in a converter can be employed [13]. Amongst them, LLC is widely used in today's DC/DC converters. Nevertheless, CLLC has its application in bidirectional power conversion systems, while LLC is efficient unidirectional resonant tank that has great efficiency under light load and therefore presents a better option than, for example, LCC for PV microinverter purposes [14].

Resonant converter with LLC tank configuration can be a MPPT stage of a two stage three phase microinverter [15]. The microinverter with galvanic isolation provides improved consumers' safety and can be appropriated for variety of PV systems' realizations [16] - [18]. Additionally, development of a dual input DC/DC converters with LLC resonant tank [19] can be considered because of its abillity to manage wide input voltage rate or it can form a scalable power conversion system as presented in [20].

This paper represents a brief overview of performance of the LLC resonant tank and design of resonant elements for a converter shown at Fig. 1 with 1000 W rated power. Full bridge is considered before resonant tank, while diode rectifier is on transformer's secondary side before DC link.

In the Section II voltage gain and load dependance of the LLC resonant tank is introduced. Following, design procedure of a tank is described with capacitor selection in Section III and inductor design in Section IV. In the last section, experimental results are presented.

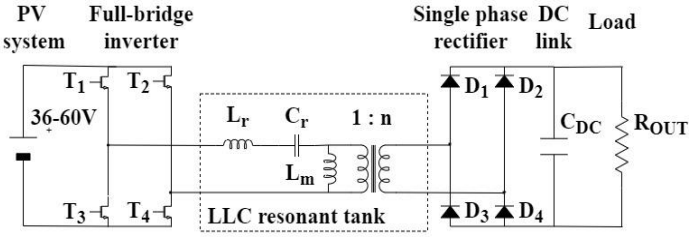

Fig. 1. Resonant LLC topology of a DC/DC converter with a passive load

II. LLC VOLTAGE GAIN AND LOAD DEPENDENCE

The design of a resonant tank requires input quantities' information including aforementioned rated power with 48 VDC input voltage as well as other parameters listed in Table I. While designing the presented system, the assumption was adopted that the output voltage of the converter will be maintained at a constant value by a proper control system.

Quality factor Q is of a great influence for the analysis of the tank. It represents the change in a converter's voltage gain curve at a different load conditions [21] and is characterized by equation (1)

$$Q = n^2 \cdot \frac{\pi^2}{8} \cdot \frac{P_{out}}{V_{out}^{\ 2}} \cdot \sqrt{\frac{L_r}{C_r}} \tag{1}$$

where P_{out} [W] is rated power, V_{out} [V] is an output voltage and n the ratio of secondary and primary number of turns. As it can be seen, Q factor is greater as the load approaches to the nominal value. Additionally, resonant frequency of the LLC resonant tank is described by

$$f_r = \frac{1}{2 \cdot \pi \cdot \sqrt{(L_r + L_m) \cdot C_r}} \tag{2}$$

L_r being series resonant inductor, C_r series resonant capacitor and L_m the magnetizing inductance of the transformer.

Voltage gain of the tank is determined by the ratio of the switching and resonant frequency, load conditions (Q factor) and inductor ratio (m) as can be seen in the following equation

$$M = \frac{1}{\sqrt{\left[1 + \frac{1}{m} - \frac{1}{m} \cdot \left(\frac{f_s}{f_r}\right)^2\right]^2 + Q^2 \cdot \left(\frac{f_s}{f_r} - \frac{f_r}{f_s}\right)^2}}. \tag{3}$$

Inductor ratio m is a constant that defines a ratio of a magnetizing inductance of a transformer L_m and series resonant inductance L_r. Increasing m value, voltage gain characteristics are more flattened thus more stable in wide frequency range, with reduced voltage peak on very light load. This effect can be seen on Fig. 2 where voltage gain characteristics are shown for a number of different Q factors and two different m values – high on the right and low one on the left.

In case m factor is high, LLC resonant tank condenses to a two-element circuit, meaning only L_r and C_r are utilized in a resonant occurrence and current through L_m is reduced. Alternating charging and discharging of the resonant capacitor and inductor leads to a reactive power exchange within these two reactive elements in the circuit which minimizes the apparent power of the tank. With reduced apparent power, the rms value of the current through the series resonant components is lowered and therefore the voltage drops, and Joule's power losses are lessened. High L_m is easily achievable and justified since transformer is there to provide galvanic isolation.

To make sure that larger deviation from the resonant frequency, due to switching frequency change, does not mitigate the voltage gain, the minimum Q factor must be established since that state could jeopardize elements bringing attenuation larger than one as seen in Fig. 2. This is because in case of light load, high values of the equivalent R_{out} could approach to similar value to $X_m = 2 \cdot \pi \cdot f \cdot L_m$ and parallel phenomena comes to the fore. The appropriate minimum Q value for the calculations must be determined knowing the expected load conditions. With all the requirements said, quality factor is taken to be 0.4.

TABLE I
INPUT PARAMETERS FOR THE DESIGN OF REACTIVE ELEMENTS

Parameter	Symbol	Value
Quality factor	Q	0.4
Turns ratio	n	11
Inductor ratio	m	100
Rated power [W]	P_{out}	1000
Input voltage range [V]	V_{in}	36 - 60
Output voltage [V]	V_{out}	450
Duty cycle	D	0.5

III. CAPACITOR SELECTION

In attempt to achieve high power density it is necessary to minimize volume of resonant elements by operating on high frequencies. However, it should be noted that working with

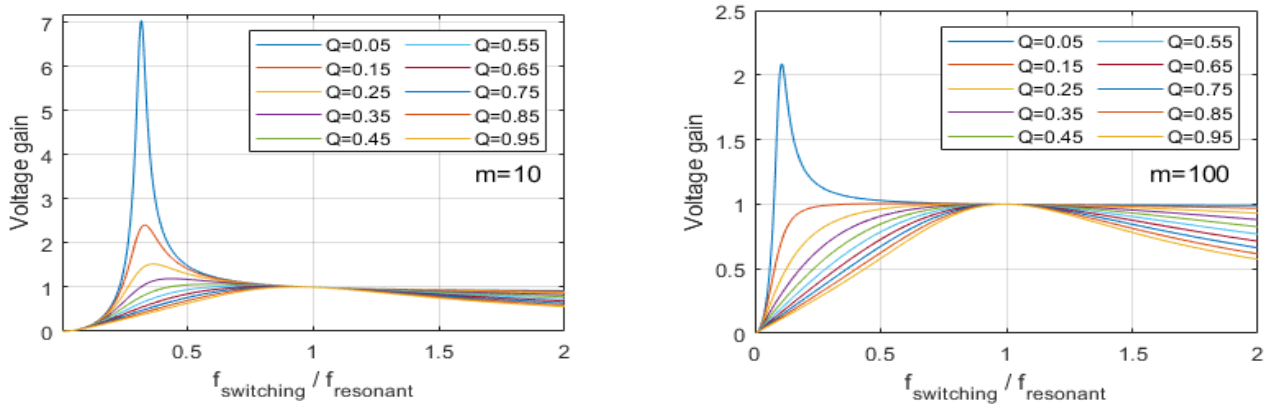

Fig. 2. LLC resonant tank voltage gain dependance on load conditions (Q) and switching frequency for two different values of m – 10 (left) and 100 (right)

too high frequencies brings other problems, for example higher switching losses on semiconductor devices. These losses are significantly lowered in LLC resonant topology due to zero voltage and zero current switching [22].

Values of resonant inductances and capacitance are related through resonant frequency f_r as show in equation (2). Capacitance as a function of frequency for agreed quality factor Q calculated using (1) and (2) is presented on Fig. 3.

An important step in the process of choosing resonant elements is to determinate frequency range in which the value of resonant capacitance stays unchanged. It has been noticed that after 150 kHz the curve portraited in Fig. 3 approximately stays in the flat region. After profound analysis of the transformer's power density, it is established that working with the frequency of 200 kHz with the chosen core material N87, volume of the transformer is sufficiently reduced.

Software simulations in LTspice were conducted applying switching frequency of 200 kHz, nominal input voltage 48 VDC, nominal active power 1 kW, capacitance value determined according to results based on Fig. 3, inductance value calculated by (2) for designated C and input parameters mentioned before. Based on simulation results in rated conditions, resonant current takes absolute value of 24 A.

From the manufacturer's documentation the one can find that an increase in resonant frequency leads to decreases in the maximum rated capacitor voltage as well as maximum rated current. Hence, further frequency rise would result in lowering capacitor's maximum rated current. It means usage of more parallel connected capacitors would be required in order not to pass maximum rated current of a single unit.

Based on the Fig. 3 for the frequency of 200 kHz, needed capacitance equals 1.327 µF. To maintain value of the capacitance for which the resonant current has the minimum value, LTspice simulations were performed. Capacitance value was changed in the range between 1 µF and 2 µF. It was necessary to secure that the current value in that range of capacitances does not fluctuate intensively for the input voltages. Minimum resonant absolute current value was 24 A, achieved in case of the capacitance value of 1.2 µF and inductance of 0.528 µH.

Since inductor will be designed according to the needs and considering the presented evaluation, selection criteria for capacitor are:

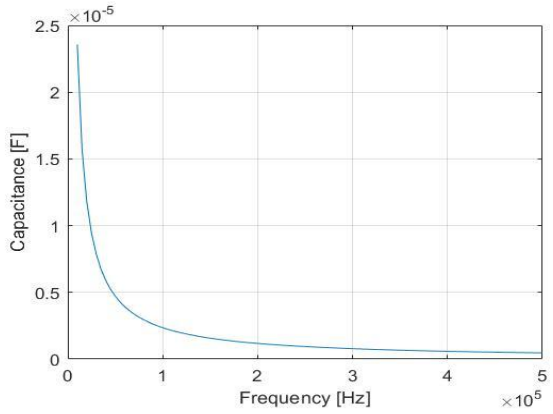

Fig. 3. Value of the resonant capacitance as a function of a resonant switching frequency

- absolute maximum current higher than 24 A on 200 kHz in case of using only one capacitor,
- low equivalent series resistance (ESR),
- capacitance value 1.2 µF,
- flat curve capacitance in a function of frequency,
- flat curve ESR in a function of frequency.

In case capacitor with these parameters is not available, possible solution would be to use more than one, i.e. x units with x times smaller capacitance rated for at least $1/x$ times of the mentioned current. However, suitable component was successfully found, so one unit can be used, and it is KEMET's film capacitor C4BSPBX4120ZB0J.

IV. Inductor Design

After established inductance value of 0.528 µH, resonant inductor can be designed. Transformer's leakage inductance is not taken into consideration as a part of the equivalent inductance since it depends on various factors such as the tightness of the windings and windings' layout. Additionally, it is expected to have very low value.

Knowing the operating frequency, appropriate material can be selected according to manufacturer's suggestion. Inductor core's shape is taken to be E due to simplicity of winding and higher availability on the market. For 200 kHz suggested materials available for E cores are N87, N95 and N97.

A. Determining the core size

Firstly, according to [23], the core's dimensional parameter, S_wS_c, which represents product of the core's cross section (S_c) and the core's window area (S_w), should be above the value calculated using the following formula

$$S_wS_c = \sqrt[7]{\left(\frac{\sqrt{1+k_\gamma}\cdot K_i\cdot L\cdot I_{peak}^2}{B_{\max}\cdot K_t\cdot\sqrt{k_u\cdot\Delta T}}\right)^8}\cdot 10^{12} \qquad (4)$$

where:

- k_γ is the ratio between core and copper losses taken to be 1,
- K_i is the current waveform constant,
- L is the needed inductance value,
- I_{peak} is the maximum current intensity,
- B_{max} is the maximum value of flux density limited by the saturating flux density,
- K_t is the constant suggested by [23] to be 48200 as the core shape is not pot type; considering this constant acknowledges the copper resistivity on 20°C, it should be scaled so that the specific electrical resistivity is the one on 100°C which is $2.3\cdot10^{-8}$ Ωm,
- k_u is window utilization factor and
- ΔT is the core temperature rise.

Resulting S_wS_c values for each material are in Table II as well as the values of each listed parameter.

Inductance value for any core can be calculated as:

$$L = A_L\cdot N^2 \qquad (5)$$

where N is the number of turns. After selecting core that has S_wS_c value higher than the one from the Table II, A_L value can be read from the core's datasheet and L calculated using (5).

However, due to high current application, it is very important to take into consideration the fact that the diameter of the conductor will be relatively big. Therefore, prior to selecting the smallest possible core in order to achieve high power density, it is important to check if the window area is large enough for the turns.

B. Determining the size of the conductor

Current density should be below 4 A/mm^2 as a good practice, and as suggested by [24]. As current will not exceed 24 A, the diameter of the conductor should be at least 2.8 mm.

Owning to high frequency, it is advisable to use litz wires. This is due to small skin depth of the high frequency current which can be calculated based on the following equation [25]

$$\delta = \sqrt{\frac{\rho_{Cu}}{\pi \cdot f \cdot \mu}} \tag{6}$$

ρ_{Cu} being the specific electrical resistance of the copper, f operating frequency in Hz and μ material's permeability. Based on (6), for 200 kHz the strand of the conductor should be below 292 μm. Due to proximity effect, it appeared that smaller strands result in better efficiency, which has also been a suggestion by litz wires' manufacturer. Finally, based on the market available wires in required quantity, selected conductor has 2800 strands of the diameter 0.072 mm.

Taking the conductor's size into consideration besides the minimum S_wS_c value from the Table II, smallest available core that has large enough window area is the core E 25/13/7. It is produced in materials N87 and N97 and it has approximate A_L value 1850 nH and 1950 nH respectfully. Still, the inductance value computed using (5) even with only one turn is too high. This can be solved by adding a gap to the core.

TABLE II
INPUT PARAMETERS AND NEEDED S_wS_c VALUES

Symbol	Parameter	N97	N87	N95
B_{sat}	Saturating flux density [T]	0.41	0.39	0.41
L	Inductance [μH]	0.52		
K_i	RMS and peak current ratio	0.707		
K_t	Core shape constant	41703		
I_{peak}	Current peak value [A]	42.43		
k_u	Window utilization factor	0.8		
ΔT	Temperature rise [°C]	70		
B_{max}	Maximum flux density [T]	0.4	0.38	0.4
S_wS_c	Core size [mm^4]	529.3	561.2	529.3

C. Determining the gap size

Inductance of the gapped core can be calculated as

$$L = \frac{N^2}{\frac{1}{\mu_0}\cdot\left(\frac{l_g}{S_c}+\frac{1}{\mu_r}\cdot\frac{l_c-l_g}{S_c}\right)} = \frac{N^2}{\frac{1}{\mu_0\cdot\mu_{eff}}\cdot\frac{l_c}{S_c}} \tag{7}$$

where l_g [mm] is the gap length, l_c [mm] the length of the flux path corresponding to the chosen core, μ_r is the material's relative permeability, μ_0 [H/mm] magnetic permeability of the air and S_c [mm^2] core's cross section. Thus, adding the air gap μ_{eff} is being shrunk and therefore N has achievable value. Additionally, air gap contributes to stability of the magnetic properties of the core [26].

The core E 25/13/7 in material N97 cannot be gapped by the manufacturer, so the chosen material is N87. The manufacturer has predefined values for air gaps: 0.1 mm, 0.16 mm, 0.25 mm, 0.5 mm, and 1 mm. In Table III it is listed how many turns is needed in case of different gap lengths. Also, the A_L value in case fringing effect is taken into consideration is given by the manufacturer and presented in Table III.

For the 0.5 mm air gap the difference in desirable and resulting A_L and μ_{eff} is the least as seen from Table III. Hence, the chosen core is E 25/13/7 in material N87 with the air gap of 0.5 mm having two turns of litz wire consisting of 2800 strands of the diameter 0.072 mm. Resulting inductance is expected to be 0.5976 μH.

TABLE III
GAPPED E 25/13/7 CORE ANALYSIS

Air gap length [mm]		0.1	0.5	1
Number of turns		1	2	3
Desired μ_{eff} value		462	115	51
Desired A_L value [nH]		530	132.5	58.9
μ_{eff}	No fringing effect	456	109	56
	With fringing effect	422	130	78
A_L [nH]	No fringing effect	523.2	125.4	64.3
	With fringing effect	484.4	149.4	90.0

D. Finite Elements Method Analysis

Using software tool FEMM 4.2 finite elements method analysis is conducted. The graphical result is shown in Fig. 4. It should be noted that the flux density in the fringes passes the saturating point.

Inductance value calculated by the software is 0.086 μH. However, this value should be scaled since FEMM 4.2, while calculating equivalent inductance, considers only the part of the turn that is inside the core window. Thus, the value given by the program should be multiplied with the ratio of the turn length in millimeters and doubled core depth, i.e. 14 mm. Corrected value equals to 0.307 μH.

V. EXPERIMENTAL RESULTS

The main intent of testing is to observe the behavior of the resonant topology. Prototype of LLC resonant DC/DC

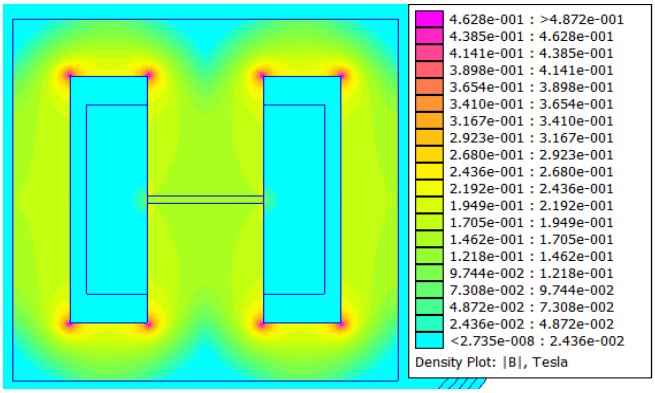

Fig. 4. Flux density in the core done in the software tool FEMM 4.2

converter for 1 kW was developed in Digital Drive Control Laboratory in School of Electrical Engineering, University of Belgrade.

Designed prototype with testing circuit is presented in Fig. 5. Prototype was realized with gallium nitrite transistors as input DC to AC converter in a full bridge configuration using two EPC1022 development boards. However, since these transistors could work with even higher frequencies and remain satisfactorily efficient, it is advisable to, but not limited to, consider them in 500 kHz or higher application. Nevertheless, they can function properly on 200 kHz as well, so they had been taken as a part of the prototype, since accent is on the resonant tank rather than full-bridge parameters.

The measured parameters of the designed and selected resonant tank elements are 0.648 μH for resonant inductance, 49.55 μH for transformer's magnetization inductance, and capacitances of 100 μF and 1.2 μF for DC link and resonant capacitor respectively with load resistance of 650 Ω. Transformer's magnetization inductance, series inductance and capacitance were measured using LRC meter, with 200 kHz excitation signals. For driving transistors in full-bridge configuration, Texas Instruments launch pad 28379D was used employing Power Width Modulation (PWM) signals with adjustable dead time duration. Soft start was necessary to implement in order to avoid unwanted impulsive changes of resonant current. It was realized by phase shift modulation of driving signals. During 3.6 s, one of PWM signal's duty cycle was changed in the range of 0 – 50 %.

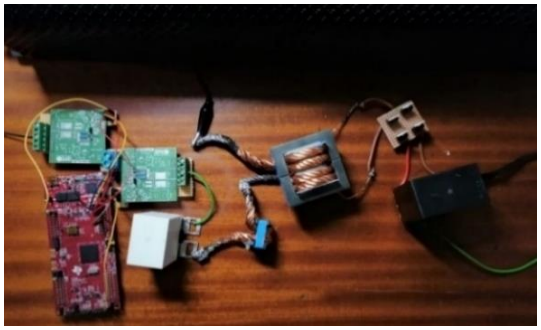

Fig. 5. Experimental setup of LLC resonant DC/DC converter

According to theoretical calculations for resonant tank parameters, switching frequency was set to 200 kHz. The voltage waveforms on primary and secondary transformer side with switching frequency of 200 kHz and 15 VDC at the input converter terminals are shown in Fig. 6. It can be noticed that the transformer's low side voltage is multiplied by the turns' ratio. Also, voltage gain of resonant tank is equal to one, as expected.

Waveform of resonant current is presented in Fig. 7 where input parameters were the same as mentioned before. Based on measurements, resonant inductance takes value of 0.648 μH instead of theoretical 0.528 μH due to imperfections of the inductor's development process. Resonant frequency was now estimated using (2) once again and set to 187 kHz.

Capacitances on the output of the diodes of the rectifier along with output capacitances of the transistors from full-bridge are not being fully discharged during the dead time. As a result, these parasitic capacitances and the circuit inductance had started to resonate, and flinches appeared. In Fig 8. these oscillations on the resonant current waveform can be noticed.

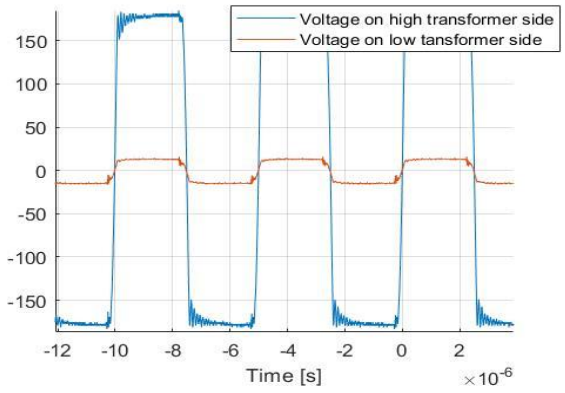

Fig. 6. Voltages on low and high transformer side with 15VDC input voltage and switching frequency of 200kHz.

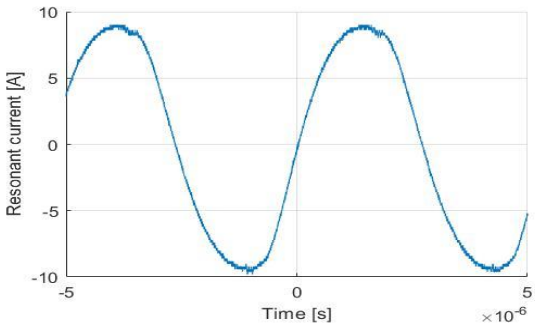

Fig. 7. Waveform of resonant current for 15 VDC input voltage and 200 kHz switching frequency

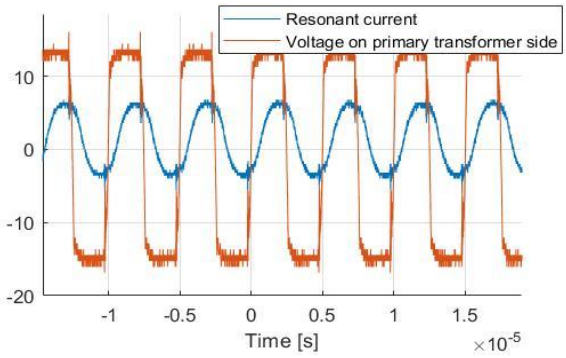

Fig. 8. Waveforms of resonant current and voltage on primary transformer side for 187 kHz as a switching frequency

VI. Conclusion

Having the advantage of reduced switching losses due to zero current and zero voltage switching, resonant DC/DC topologies are worth considering in the high frequency high current application in PV inverters. Numerous resonant tank topologies are possible, where LLC is the most common one in the terms of voltage gain stability and design simplicity.
In this paper the process of determining needed series capacitance and inductance's values from LLC resonant tank is presented. Transformer's magnetization inductance has 100 times larger value, so its impact has been neglected.

Thereafter, the procedure of choosing capacitor and inductor design is elaborated in detail.

On the developed prototype, waveforms of relevant variables were observed in a resonant circuit in order to verify the presented design procedure. Experimental tests have shown that the presented method gives satisfactory results in terms of the system's behavior. The resonant LLC converter, in addition to the possibility of working in MPPT mode and galvanic isolation, provides high efficiency and power density, thus reducing the volume and increasing the total efficiency of the conversion system. Due to aforesaid advantages, the presented resonant tank topology is a good choice for the needs of microinverter PV applications.

Further research could take into consideration other core shapes for inductor, include transformer's leakage inductance into calculations, as well as the analysis of higher working frequencies suitable for wide-bandgap devices.

ACKNOWLEDGMENT

We would like to express special gratitude to Efficient Power Conversion (EPC) company. Their generous donation of EPC1022 development boards has helped us to undertake this project and present experimental research that we have accomplished in the Laboratory.

References

[1] R. W. Erickson, D. Maksimović in *"*Principles of Steady State Converter Analysis" *Fundamentals of Power Electronics*, New York, United States of America: Soringer, 2001, ch. 2, sec 3. pp. 22-27

[2] R. W. Erickson, D. Maksimović in *"*Steady-State Equivalent Circuit Modeling, Losses, and Efficiency" *Fundamentals of Power Electronics*, New York, United States of America: Soringer, 2001, ch. 3, sec 4. pp. 50-52

[3] S. N. Soheli, G. Sarowar, M. A. Hoque and M. S. Hasan, "Design and Analysis of a DC -DC Buck Boost Converter to Achieve High Efficiency and Low Voltage Gain by using Buck Boost Topology into Buck Topology," *2018 International Conference on Advancement in Electrical and Electronic Engineering (ICAEEE)*, 2018, pp. 1-4

[4] S. Cuk, R. D. Middlebrook, "A new optimum topology switching DC-to-DC converter" in *IEEE Power Electronics Specialist Conference*, Palo Altro, CA., USA, 1977.

[5] Y. Konishi, Y.-F. Huang, M.-J. Hseih, "Utility-interactive high-frequency flyback transformer link three-phase inverter fir photovoltaic AC module" in *35th Annual Conference of IEEE Industrial Electronics*, Porto, Portugal, 2009.

[6] Z. Chen, Q. Wu and Y. Yuan, "A Novel Zero-Voltage-Switching Push–Pull High-Frequency-Link Single-Phase Inverter," in *IEEE Journal of Emerging and Selected Topics in Power Electronics*, vol. 4, no. 2, pp. 421-434, June 2016.

[7] A. Hillers, D. Christen and J. Biela, "Design of a Highly efficient bidirectional isolated LLC resonant converter," 2012 15th International Power Electronics and Motion Control Conference (EPE/PEMC*)*, 2012.

[8] K. Siebke and R. Mallwitz, "Operation Mode Analysis of the CLLC Resonant Converter," *2019 IEEE 13th International Conference on Compatibility, Power Electronics and Power Engineering (CPE-POWERENG)*, 2019, pp. 1-6

[9] Y. Zhuang, F. Liu, X. Zyang, X. Diao, J. Jiang and J. Sun, "Direct Frequency Control Based MPPT Algorithm of LLC Resonant Converter for Photovoltaic System" in *2019 IEEE Energy Conversion Congress and Exposition (ECCE)*, Baltimore, Maryland, USA, 2019.

[10] Hillers, A., Christen, D., & Biela, J. (2012). *Design of a Highly efficient bidirectional isolated LLC resonant converter. 2012 15th International Power Electronics and Motion Control Conference (EPE/PEMC)*, 2012.

[11] F. Musavi, M. Craciun, M. Edington, W. Eberle, and W. G. Dunford, "Practical design considerations for a LLC multi-resonant DC-DC converter in battery charging applications," in Proc. 27th Annu IEEE APEC Expo., 2012, pp. 2596–2602

[12] R. L. Steigerwald, "A comparison of half-bridge resonant converter topologies," in *IEEE Transactions on Power Electronics*, vol. 3, no. 2, pp. 174-182, April 1988.

[13] R. Severns, "Topologies for three element resonant converters," Fifth Annual Proceedings on Applied Power Electronics Conference and Exposition, 1990, pp. 712-722

[14] S. Mao, J. Popovic, R. Ramabhadran and J. A. Ferreira, "Comparative study of half-bridge LCC and LLC resonant DC-DC converters for ultra-wide output power range applications" *2015 17th European Conference on Power Electronics and Applications (EPE'15 ECCE-Europe)*, 2015, pp. 1-10

[15] Alamir, O. Abdel-Rahim, M. Orabi and M. Ismeil, "Two-Stage Resonant Three-Phase Micro-inverter for Grid-Tie PV Application," *2019 IEEE Conference on Power Electronics and Renewable Energy (CPERE)*, 2019, pp. 459-464

[16] G. Rubino, L. Rubino, N. Serbia, P. Ladoux and P. Marino, "LLC resonant converters in PV applications comparison of topologies considering the transformer design," *2013 International Conference on Clean Electrical Power (ICCEP)*, 2013, pp. 37-41

[17] C. Buccella, C. Cecati, H. Latafat and K. Razi, "A grid-connected PV system with LLC resonant DC-DC converter," *2013 International Conference on Clean Electrical Power (ICCEP)*, 2013, pp. 777-782

[18] A. Bousselham and A. Elrayyah, "Control and efficient operation of low cost multi PV-based LLC resonant microinverters," *2016 IEEE 43rd Photovoltaic Specialists Conference (PVSC)*, 2016, pp. 3457-3462

[19] S. M. Tayebi, H. Hu, O. Abdel-Rahman and I. Batarseh, "Design and analysis of a dual-input single-resonant tank LLC converter for PV applications," *2018 IEEE Applied Power Electronics Conference and Exposition (APEC)*, 2018, pp. 476-483

[20] C. Schaef and J. T. Stauth, "Multilevel Power Point Tracking for Partial Power Processing Photovoltaic Converters," in *IEEE Journal of Emerging and Selected Topics in Power Electronics*, Dec. 2014, vol. 2, no. 4, pp. 859-869

[21] G. Hsieh, C. Tsai and S. Hsieh, "Design Considerations for LLC Series-Resonant Converter in Two-Resonant Regions," *2007 IEEE Power Electronics Specialists Conference*, 2007, pp. 731-736

[22] X. Zhou, Z. Liang and A. Huang, "A High-Dynamic Range Current Source Gate Driver for Switching-Loss Reduction of High-Side Switch in Buck Converter," in IEEE Transactions on Power Electronics, June 2010. vol. 25, no. 6, pp. 1439-1443

[23] W. G. Hurley, W. H. Wölfle, "Inductor Design," in *Transformers and Inductors for Power Electronics*, Chichester, United Kingdom: John Wiley & Sons Ltd., 2013, ch. *3*, sec. *1-2*, pp. *61-64*

[24] A. I. Pressman, K. Billings, T. Morey, "Transformers and Magnetics Design," in Switching Power Supply (3th Edtion), New York, United States of America: McGraw Hill Education, 2013, ch. *7*, sec. 3, p. *313*.

[25] A. V. Bossche, V. C. Valchev, "Soft Magnetic Materials" in *Inductors and Transformers for Power Electronics*, Boca Raton, United States of America: CRC Press Taylor & Francis Group, 2005, ch. *3*, sec. *3*, pp. *136–137*

[26] W. G. Hurley, W. H. Wölfle, "Inductance," in *Transformers and Inductors for Power Electronics*, Chichester, United Kingdom: John Wiley & Sons Ltd., 2013, ch. *2*, sec. *1*, pp. *25–38*